Uluslararası İleri Doğa Bilimleri ve Mühendislik Araştırmaları Dergisi
Sayı 8, S. 343-352, 9, 2024

Araştırma Makalesi

IJANSER
https://as-proceeding.com/index.php/ijanser
ISSN:2980-0811

International Journal of Advanced Natural Sciences and Engineering Researches
Volume 8, pp. 343-352, 9, 2024

Research Article

Tooth Root Stress Relief Hole Optimization on the Spur and Helical Gears

Efe Savran[1], Fatih Karpat[1]
[1] *Mechanical Engineering Department, Bursa Uludag University, 16059, Bursa, Turkey*
E-Mail: efesavran@uludag.edu.tr, karpat@uludag.edu.tr

(Received: 16 October 2024, Accepted: 27 October 2024)

(4th International Conference on Engineering, Natural and Social Sciences ICENSOS 2024, 22-23 October 2024)

ATIF/REFERENCE: Savran, E. & Karpat, F. (2024). Tooth Root Stress Relief Hole Optimization on the Spur and Helical Gears, *International Journal of Advanced Natural Sciences and Engineering Researches*, 8(9), 343-352.

Abstract-In this study, optimal design and placement of tooth root stress-relieving holes in spur and helical gears were made. 3-dimensional models of a spur gear with a module of 3 and several teeth of 20 a helical gear with the same dimensions and a helical gear with a helix angle of 15 degrees were created in SolidWorks. 8 different hole combinations were added to the gear models and included in the static analysis in ANSYS with the same boundary conditions. In the finite element analyses, general gear stress distribution, tooth root stress distribution, and deformation results were obtained. According to the findings, a 1.25 mm diameter hole opened on a 50 mm diameter circle gave the most successful result in reducing spur gear tooth root stress and gear mass. However, an effective result could not be obtained in the helical gear.

Keywords: Involute Spur Gear, Stress Relief Hole, Tooth Root Stress, Finite Element Analysis, Gear Design.

I. INTRODUCTION

There is a great deal of use for gears in industries such as automotive, aerospace, machinery, and energy [1]. While they are used in macro places such as ships and wind turbines, they are also used in micro-electromechanical systems (MEMS). The main purpose is to transfer torque and speed between two different shafts with periodic rigidity. The torque transferred may vary with the change in gear design. In this way, efficiency issues are also addressed. The most well-known example of this is automobile gearboxes. By preparing gear sets with different transmission ratios, the necessary performance and driving efficiency can be achieved in a moving automobile. On the other hand, gearboxes in wind turbines are also very important in the energy sector. The speed created by the wind force moving the turbine blades is changed with a gearbox prepared with certain gear ratios and transmitted to the electric generator and electrical energy is obtained.

Machines and systems operate more efficiently, reliably, and efficiently when gears are designed properly. The incorrect design of a gear can lead to excessive wear, noise, vibration, energy loss, and failure very quickly. It is important to note that an incorrect gear design can negatively affect torque transmission in applications requiring a high level of torque and speed. This will also lead to mechanical components wearing out more quickly and increase maintenance costs. Furthermore, there are a number of factors that determine the durability and performance of gears, ranging from the choice of material to the design of the gear. In the case of a well-designed gear system, the efficiency of the system is maximized, the amount of energy lost is minimized, and thus the overall performance is improved.

Finite Element Analysis (FEA) is a numerical method that can provide predictions for mechanical behavior [2]. It includes methods such as static analysis, fatigue analysis, noise, vibration, harshness (NVH) analysis. It is also a method used in many studies in terms of gear analysis. It enables optimizations that increase product life by showing the mechanical behavior of gears under loading in detail [3]. It also helps in selecting the appropriate material for the structure. Side surface and tooth root strength are taken into consideration in the strength and life examination of gears. FEA shortens the optimal gear design processes by providing a highly sensitive and high-accuracy stress distribution.

Opening stress relief holes in gears is a method used to reduce stress accumulations at the tooth roots [4]–[6]. Stress relief holes are strategically designed and placed to extend the life of the gear and increase its safety by reducing stress accumulations at the tooth roots during operation. Thanks to the holes, stress concentration in weak areas is reduced and the risk of cracks is minimized. At the same time, stress relief holes provide a lightening of gear weight and material savings. For optimal design, the size, location, and number of holes should be determined with great care. Inappropriate hole location and size may reduce gear strength and lead to unexpected structural failures. Therefore, stress and deformation distributions before and after opening stress relief holes should be examined in FEA models.

II. MATERIALS AND METHODS

In this study, dimensional and positional determination of stress relief holes opened on an involute gear was carried out. For this purpose, gear design and FEA boundary conditions in the references [7], [8] and [9] were taken into consideration. Tooth root stress was calculated with the numerical equation for the spur and helical gear with known design features and loading conditions. Then, the FEA model was constructed, and maximum stress values were examined in terms of consistency. The helical gear is a 15-degree helix angle version of the spur gear whose design features are included in the references. Combinations including the diameter and location of stress relief holes were created. Hole combinations were added to the gear 3-dimensional model and included in the static analysis with the same FEA boundary conditions. The resulting gear masses, maximum tooth root stresses, and maximum deformation were compared and the stress relief hole with the most optimal combination was determined. Table 1 includes the design parameters of the involute spur gear examined in the study.

Table 1. Dimensional variables of the gear

Design Parameters	**Symbol**	**Value**	**Unit**
Module	m	3	mm
Number of teeth	z	20	-
Pressure angle	α	20	degree
Addendum	h_a	1xm	mm
Dedendum	h_f	1.25xm	mm
Tip radius of the cutter		0.47xm	mm
Profile shifting	x	0	mm
Face width	b	24	mm
Hole diameter		10	mm
Material		16MnCr5	-

According to the gear design and loading conditions in the relevant references, a torque of 100 Nm was applied to the gear center. The tangential force was calculated as 3333 N, and the normal force on the tooth flank surface was calculated as 3546 N. The calculation of the normal force is given in Equation 1. Here, M is the torque to which the gear is exposed, and D_0 is the pitch circle diameter obtained by multiplying the module and the number of teeth.

$$F_n = \frac{M}{\frac{D_0/2}{\cos \alpha}} \quad (1)$$

Figure 1 shows the tangential (Ft) and normal forces (Fn) on the pitch circle of a spur gear and the tangential, radial (Fr), and axial forces (Fe) on a helical gear when a torque of 100 Nm is applied. Force calculations are given in Equation 2.

$$D_h = \frac{m\,z}{\cos \beta}$$
$$F_t = \frac{M}{D/2} \quad (2)$$
$$F_r = F_t \tan\alpha$$
$$F_e = F_t \sin\beta$$

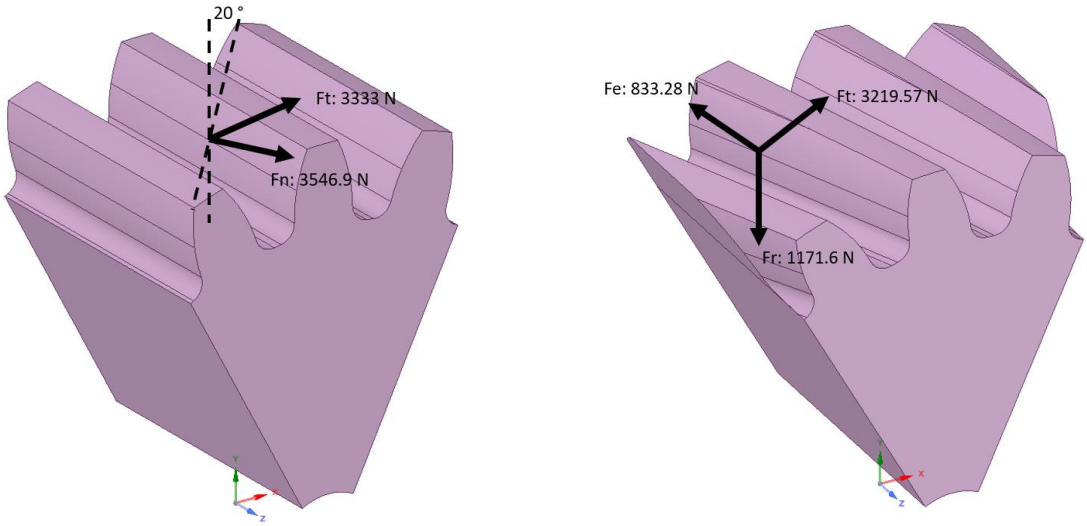

(a) (b)

Figure 1. Force definition; (a) spur gear, (b) helical gear

Equation 2 includes calculating the stress at the root of a tooth in MPa. Tooth form factor Y_{Fa} is taken as 2.85, notch sensitivity factor Y_{Sa} is 1.55, contact ratio factor Y_ε is 0.71, helix angle factor Y_β is 1, application factor K_A is 1, dynamic factor K_v is 1.02, face load distribution factor $K_{F\beta}$ is 1.116, transverse load distribution factor $K_{F\alpha}$is 1. In addition to these data, when the design parameter values in Table 1 are included, the spur gear tooth root stress value is calculated as 159.94 MPa.

$$\sigma_F = \left(Y_{Fa} Y_{Sa} Y_\varepsilon Y_\beta \frac{F_t}{b m_n}\right) K_A K_v K_{F\beta} K_{F\alpha} \quad (2)$$

Equation 3 shows the gear contact ratio calculation during the operation of two gears with a transmission ratio of 1 whose design parameters are given in Table 1. Considering the values in Table 1 for addendum radii ra1 and ra2, base circle radii rb1 and rb2, contact angle a, and distance between gear axes ad, the contact ratio is calculated as 1.627.

$$\varepsilon_\alpha = \frac{\sqrt{r_{a1}^2 - r_{b1}^2} + \sqrt{r_{a2}^2 - r_{b2}^2} - a_d \sin\alpha}{\pi\, m \cos\alpha} \quad (3)$$

In addition to the parameters used in spur gear, the tooth root stress calculation for helical gear, helix angle factor Y_β is 0.68, the normal module was calculated as 2.897 mm according to Equation 4, the helical overlap ratio is 0.68 from Equation 5, and the total contact ratio on the helical gear was found as 2.307 according to Equation 6. Helical gear tooth root stress was calculated as 111.07 MPa.

$$m_n = m_t \cos\beta \quad (4)$$

$$\varepsilon_\beta = \frac{b \sin\beta}{\pi\, m_n} \quad (5)$$

$$\varepsilon_T = \varepsilon_\beta + \varepsilon_\alpha \quad (6)$$

Finite Element Model

The gear model, whose design parameters and boundary conditions are given in the relevant references, was created in SolidWorks 2022 according to the involute gear design rules. The 54-degree part of the gear model to be included in the FEA was knitted with a 0.3 mm hexahedral mesh element. Figure 2 shows the mesh structures of the spur and helical gears. Mesh metrics were shared in Table 2.

Table 2. Mesh details of the gears

Mesh metrics	**Spur gear**	**Helical gear**
Nodes	1442049	1485845
Elements	369816	393097
Average skewness	0.1755	0.2285
Average aspect ratio	1.9477	2.2079
Average element quality	0.8786	0.84779
Average orthogonal quality	0.8938	0.85252

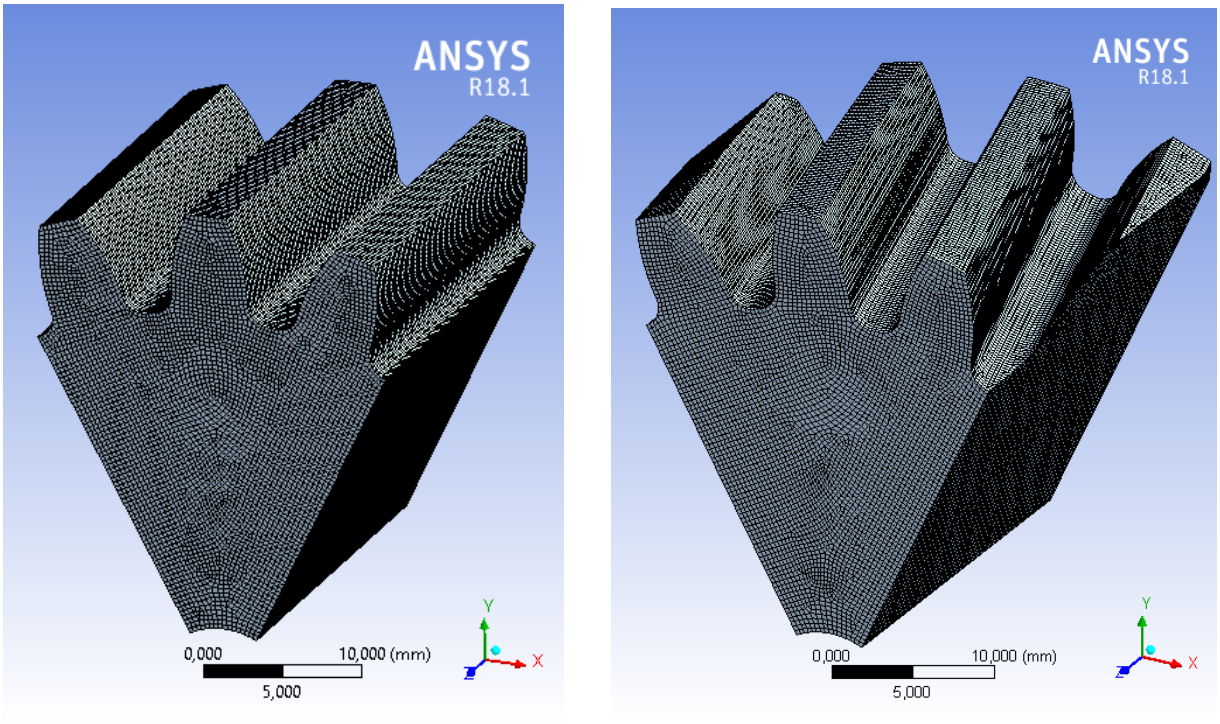

(a) (b)

Figure 2. Gear structure models; (a) spur gear, (b) helical gear

Figure 3 shows the boundary conditions of the FEA model. The gear model was subjected to static analysis in the ANSYS 18.1 version. The normal force on the pitch circle was applied linearly along the tooth width of 3546 N for the spur gear and 3513 N for the helical gear. Fixed support was applied to the cross-sectional and center-hole surfaces of the 3 teeth models.

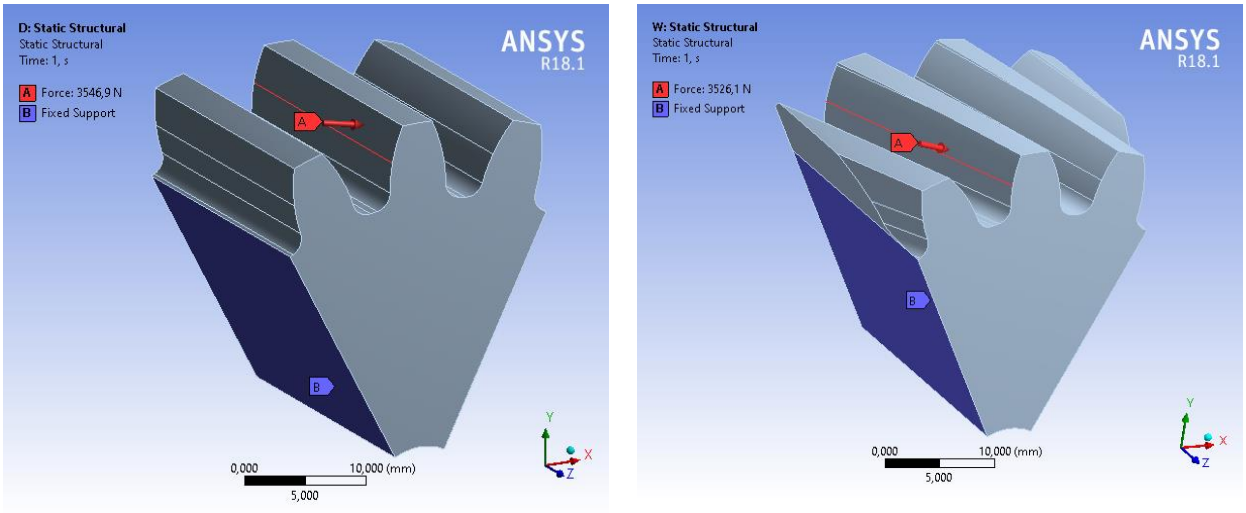

(a) (b)

Figure 3. Boundary conditions of the FEA model; (a) spur gear, (b) helical gear

Stress Relief Hole Combinations

8 different combinations were created to determine the optimal diameter and location for the tooth root stress relieving hole. The circle diameter where the hole will be placed on the gear was determined as 45 to 50 mm. The hole diameter was increased by 0.25 mm from 0.75 mm to 1.5 mm. The hole combinations are shown in Table 3. Figure 4 includes an example representation of the hole's location circle and diameter.

Table 3. Stress relief hole combinations

Combination	Placement circle diameter (mm)	Hole diameter (mm)
1	50	0.75
2	50	1
3	50	1.25
4	50	1.5
5	45	0.75
6	45	1
7	45	1.25
8	45	1.5

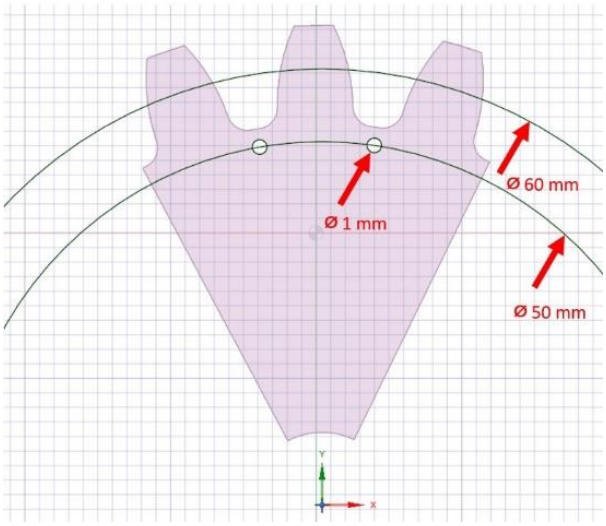

Figure 4. Stress relief hole placement example

III. RESULTS

In this study, where the optimal stress relief hole was determined with the help of FEA, the FEA results of the sur and helical gears under 100 Nm loading before the hole was added are shown in Figure 5. The maximum stress values of the tooth root of the spur and helical gears are 149.29 MPa and 117.23 MPa, and the maximum deformation values are 0.0063104 mm and 0.0070457 mm, respectively. Stresses of 730.5 MPa and 1360.5 MPa occurred on the side surfaces. The tooth root stress value obtained in the FEA model is very close to the stress value obtained from Equation 2, with a difference of 6.2% for the spur gear and 5.4% for the helical gear. Defined difference was considered acceptable, and it was seen that the setup had sufficient accuracy.

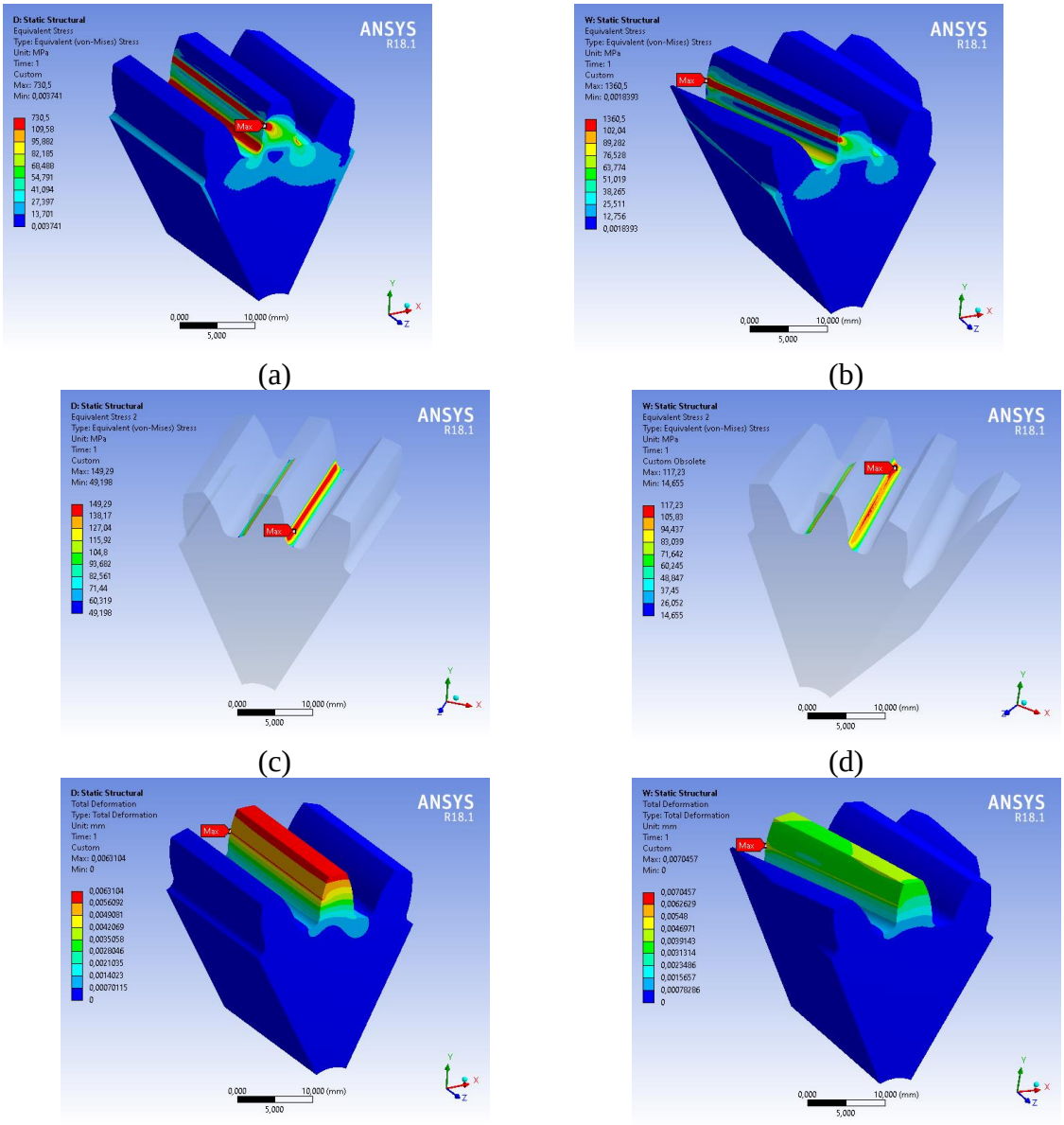

Figure 5. FEA results of the gear under the 100 Nm;
(a) stress distribution on spur gear, (b) stress distribution on helical gear, (c) tooth root stress distribution on spur gear, (d) tooth root stress distribution on helical gear, (e) deformation distribution on spur gear, (f) deformation distribution on helical gear

Figures 6, 7, and 8 show the FEA results of the effects of tooth root stress reduction holes opened in spur and helical gears. For spur gear, the 50-1.25 combination managed to reduce the tooth root stress from 149.29 MPa to 144.61 MPa. An increase in the deformation value was also observed with the increase in hole diameter. Deformation values increased to higher levels as the hole center approached the tooth root circle. A decrease in gear mass occurred with the increase in hole diameter. According to these results, opening 1.25 mm holes on a 50 mm diameter circle on the spur gear face surface will reveal the most suitable gear design. The same hole combination was not effective in reducing tooth root stress for helical gears. Deformation values increased in parallel with the increase in hole diameter. The gear mass decrease is similar to the behavior in spur gears.

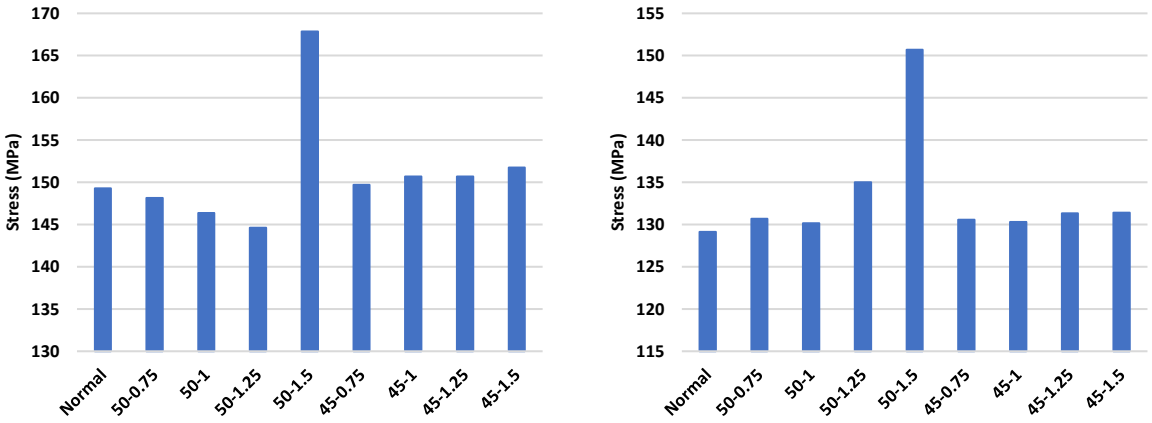

Figure 6. Maximum tooth root stress of the hole combinations; (a) spur gear, (b) helical gear

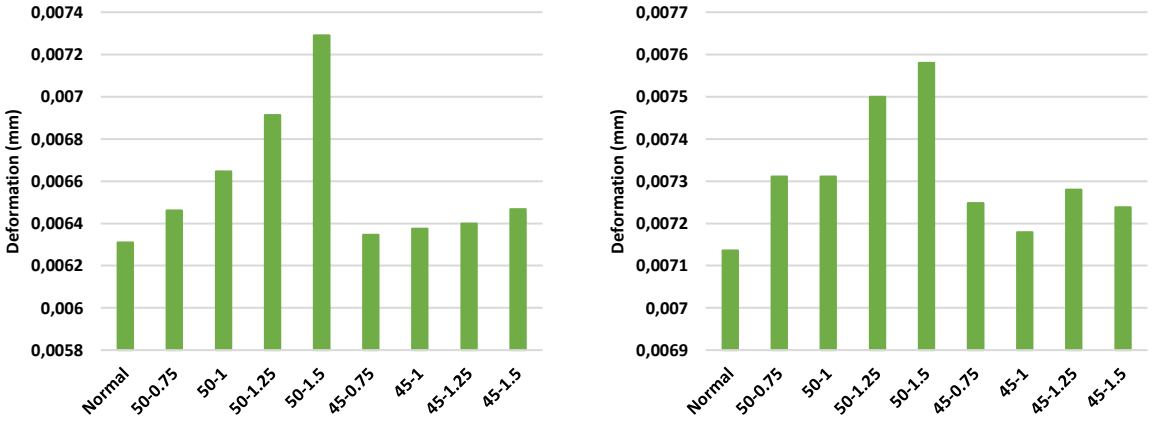

Figure 7. Maximum deformation of the hole combinations; (a) spur gear, (b) helical gear

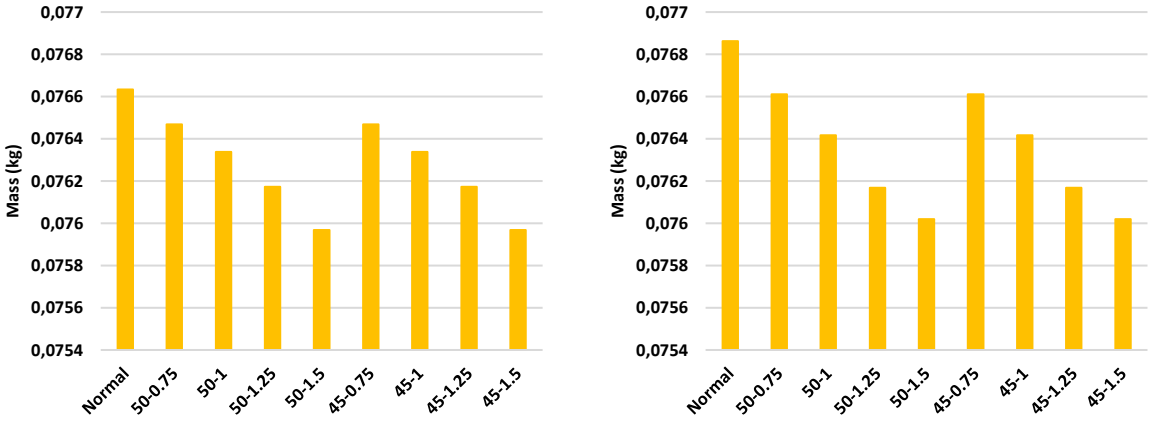

Figure 8. Gear mass variation of the hole combinations; (a) spur gear, (b) helical gear

Figure 9 shares FEA result images of a spur gear with a 50-1.25 hole combination.

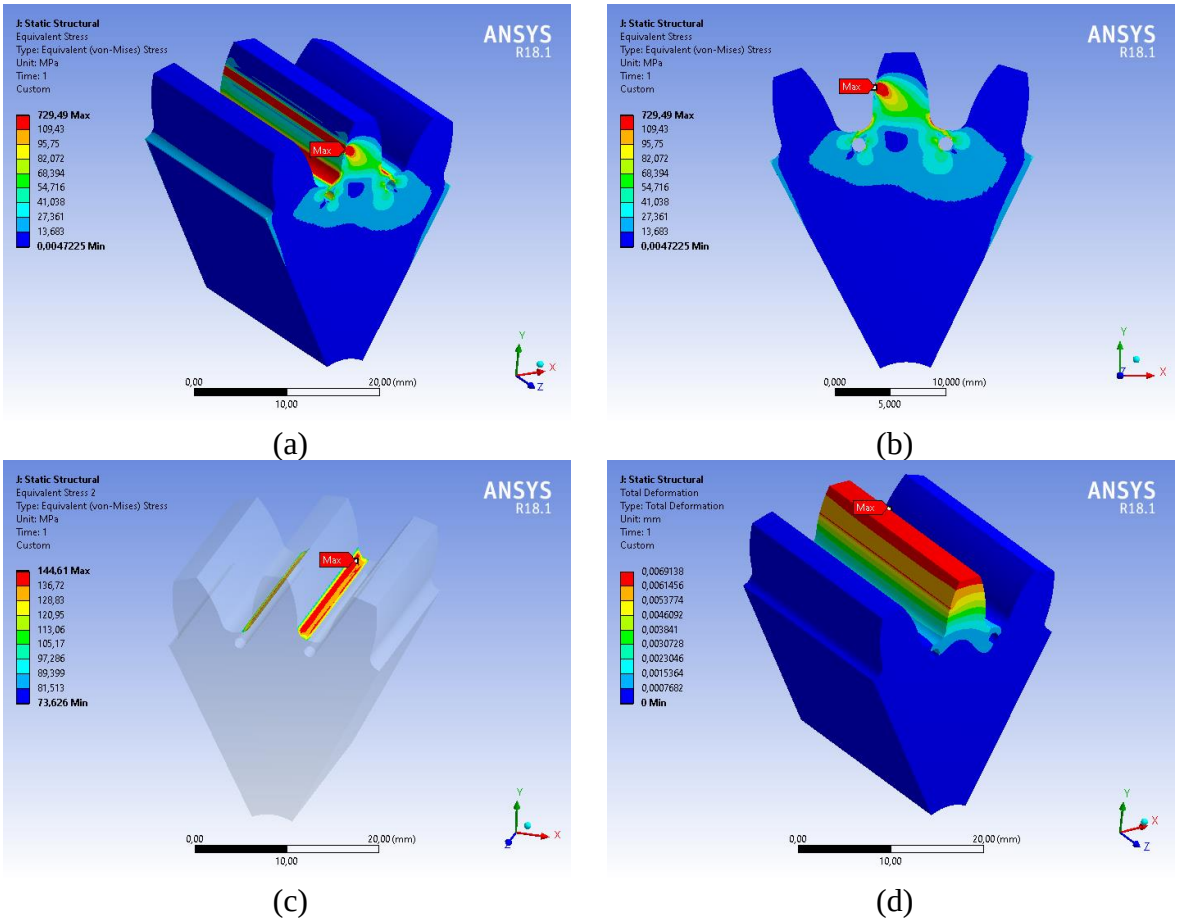

Figure 9. FEA results of hole drilled gear; (a) cross view of stress distribution, (b) frontal view of the stress distribution, (c) tooth root stress of the gear, (d) deformation distribution of the gear

REFERENCE

[1] T. G. Yılmaz, O. Doğan, and F. Karpat, "A comparative numerical study of forged bi-metal gears: Bending strength and dynamic response," *Mech. Mach. Theory*, vol. 141, no. 1, pp. 117–135, 2019, doi: 10.1016/j.mechmachtheory.2019.07.007.

[2] O. Doğan, T. G. Yılmaz, and F. Karpat, "Stress analysis of involute spur gears with different parameters by finite element and graphical method," *J. Fac. Eng. Archit. Gazi Univ.*, vol. 33, no. 4, pp. 1493–1504, 2018, doi: 10.17341/gazimmfd.416445.

[3] T. G. Yılmaz and F. Karpat, "The Effect of Tooth Thickness on Root Stress of Internal Spur Gear Mechanism," *Int. Res. J. Eng. Technol.*, vol. 6, no. 11, pp. 2079–2083, 2019, doi: 10.1177/0954406220982007.

[4] V. Pham, G. Wen, and H. Yin, "Optimization Design for Spur Gear with Stress-Relieving Holes Optimization Design for Spur Gear with," *Int. J. Comput. Methods*, vol. 12, no. 2, pp. 1–11, 2015, doi: 10.1142/S0219876215500061.

[5] R. K. Rathore and A. Tiwari, "Bending Stress Analysis & Optimization of Spur Gear," *Int. J. Eng. Res. Technol.*, vol. 3, no. 5, pp. 2044–2049, 2014, [Online]. Available: https://www.researchgate.net/publication/332187314

[6] A. S. Dhavale and A. Utpat, "Study of Stress Relief Features at Root of Teeth of Spur Gear," *Int. J. Eng. Res. Appl.*, vol. 3, no. 3, pp. 895–899, 2013.

[7] T. G. Yılmaz, O. Doğan, and F. Karpat, "A numerical investigation on the hybrid spur gears: Stress and dynamic analysis," *J. Mech. Eng. Sci.*, vol. 236, no. 1, pp. 354–369, 2022, doi: 10.1177/0954406220982007.

[8] T. G. Yılmaz, G. Karadere, and F. Karpat, "A Numerical Analysis of Hybrid Spur Gears with Asymmetric Teeth: Stress and Dynamic Behavior," *Machines*, vol. 10, no. 11, pp. 1–25, 2022, doi: 10.3390/machines10111056.

[9] F. Karpat, 2005. "Asimetrik Evolvent Dişe Sahip Düz Dişli Çarkların Analizi". Doktora Tezi, Uludağ Üniversitesi Fen Bilimleri Enstitüsü.